

SHOCK-INITIATED IMPLOSION OF AN ELLIPTICAL
CAVITY AND DETONATION IN A LIQUID LAYER

É. I. Andriankin, V. K. Bobolev,
and A. V. Dubovik

UDC 532.595.2

Many papers [1-9] have been devoted to the dynamical analysis of bubble implosion in a liquid layer. Experiments have shown that an initially circular cavity is displaced or transformed into an elliptical cavity during the implosion process due to instability, whereupon its further contraction produces cumulative jets. This problem is important in the study of surface wear in cavitation flow [7] and in the analysis of the impact sensitivity of liquid explosives [1-6]. The onset of accumulation is conveniently investigated by starting with an elliptical cavity or by displacing a circular cavity relative to the impact axis, thereby creating an asymmetrical pressure field about the center of the cavity. In the present article certain theoretical notions are advanced with regard to the onset of the cumulative jet in an elliptical or displaced cavity and its influence on the ignition of liquid explosives due to the formation of minute droplets [4] in the adiabatically heated gas inside the cavity. Experimental data on the jet formation time and the frequency of nitroglycerin detonations qualitatively support the theoretical predictions.

Consider a uniaxial impact with velocity $w_0 < 0$ by an incompressible elliptical striker having semi-axes A and B on a thin layer of incompressible viscous liquid, $h_0/A \ll 1$, which has at its center an elliptical cavity with semi-axes a and b and the same focal length as the striker, i.e.,

$$A^2 - B^2 = a^2 - b^2 = c^2$$

We assume that the mass of the load is much greater than the liquid mass, so that the layer is compressed at a constant velocity.

For small Reynolds numbers

$$Re = \rho u_0 A / \mu, \quad u_0 \sim w_0 A / h$$

the motion of the liquid in the thin layer is described by the set of theoretical lubrication equations, which is written as follows in elliptical coordinates:

$$\frac{1}{\mu H} \frac{\partial p}{\partial \alpha} = \frac{\partial^2 u_\alpha}{\partial z^2}, \quad \frac{1}{\mu H} \frac{\partial p}{\partial \beta} = \frac{\partial^2 u_\beta}{\partial z^2}, \quad \frac{\partial p}{\partial z} = 0 \quad (1)$$

$$\frac{\partial u_\alpha H}{\partial \alpha} + \frac{\partial u_\beta H}{\partial \beta} + H^3 \frac{\partial w}{\partial z} = 0, \quad H^2 = \frac{c^2}{2} (\operatorname{ch} 2\alpha - \cos 2\beta) \quad (2)$$

The variables α and β are related to the Cartesian coordinates by the familiar expressions

$$x = c \operatorname{ch} \alpha \cos \beta, \quad y = c \operatorname{sh} \alpha \sin \beta$$

The boundary conditions for these equations are represented by the conditions for adhesion to solid surfaces

Moscow. Translated from *Zhurnal Prikladnoi Mekhaniki i Tekhnicheskoi Fiziki*, No. 5, pp. 78-85, September-October, 1971. Original article submitted November 30, 1970.

© 1974 Consultants Bureau, a division of Plenum Publishing Corporation, 227 West 17th Street, New York, N. Y. 10011. No part of this publication may be reproduced, stored in a retrieval system, or transmitted, in any form or by any means, electronic, mechanical, photocopying, microfilming, recording or otherwise, without written permission of the publisher. A copy of this article is available from the publisher for \$15.00.

$$\begin{aligned} u_\alpha = 0, \quad u_\beta = 0, \quad w = w_0 \quad \text{at} \quad z = h \\ u_\alpha = 0, \quad u_\beta = 0, \quad w = 0 \quad \text{at} \quad z = 0 \end{aligned} \quad (3)$$

zero-valuedness of the tangential stresses $\sigma_{\alpha\beta} = 0$ at the cavity boundaries

$$\sigma_{\alpha\beta} = \mu \left(\frac{\partial u_\alpha / H}{\partial \beta} + \frac{\partial u_\beta / H}{\partial \alpha} \right)$$

and equality of the normal stresses $\sigma_{\alpha\alpha}$ and pressure in the gas

$$\begin{aligned} \sigma_{\alpha\alpha}(\alpha_0, \beta) = -p_0, \quad \sigma_{\alpha\alpha}(\alpha_1, \beta) = -p_1 \\ \sigma_{\alpha\alpha} = -p + 2\mu \left(\frac{1}{H} \frac{\partial u_\alpha}{\partial \alpha} + \frac{u_\beta}{H^2} \frac{\partial H}{\partial \beta} \right) \end{aligned}$$

Assuming, however, that the derivatives with respect to α and β are small, we replace these requirements with the following approximate conditions for the pressures:

$$\begin{aligned} p = p_0 \quad \text{at} \quad \alpha = \alpha_0 = \text{Arch } a / c \\ p = p_1 \quad \text{at} \quad \alpha = \alpha_1 = \text{Arch } A / c \end{aligned} \quad (4)$$

Expressing the velocities in terms of the pressure gradient from (1) and taking (3) into account, we find

$$u_\alpha = -\frac{\eta(1-\eta)h^2}{2\mu H} \frac{\partial p}{\partial \alpha}, \quad u_\beta = -\frac{\eta(1-\eta)h^2}{2\mu H} \frac{\partial p}{\partial \beta}, \quad \eta = \frac{z}{h} \quad (5)$$

Substituting these relations into the equation of continuity (2), we obtain

$$\frac{\partial^2 p}{\partial \alpha^2} + \frac{\partial^2 p}{\partial \beta^2} = -KH^2, \quad w = w_0 \eta^2 (3 - 2\eta), \quad K = \frac{12\mu |w_0|}{h^3} \quad (6)$$

We seek the solution of the Poisson equation for the pressure in the form

$$\begin{aligned} p = p_1 + A_0 + B_0 \alpha + C_0 \text{ch} 2(\alpha - \alpha_0) \cos 2\beta + D_0 \text{ch} 2(\alpha - \alpha_1) \cos 2\beta \\ p_1 = -1/8 Kc^2 (\text{ch} 2\alpha + \cos 2\beta) \end{aligned} \quad (7)$$

Evaluating the constants A_0 , B_0 , C_0 , and D_0 from condition (4) and recognizing the independence of the pressure from β at the layer boundaries, we have

$$\begin{aligned} p = \frac{(\alpha_1 - \alpha) p_0 + (\alpha - \alpha_0) p_1}{\alpha_1 - \alpha_0} + \frac{Kc^2}{8} \frac{\alpha_1 \text{ch } 2\alpha_0 - \alpha_0 \text{ch } 2\alpha_1}{\alpha_1 - \alpha_0} \\ + \frac{\alpha Kc^2 \text{ch } 2\alpha_1 - \text{ch } 2\alpha_0}{8(\alpha_1 - \alpha_0)} + \frac{Kc^2 \text{ch } 2(\alpha - \alpha_0) + \text{ch } 2(\alpha - \alpha_1)}{8(1 + \text{ch } 2(\alpha_1 - \alpha_0))} \cos 2\beta \\ - 1/8 Kc^2 (\text{ch } 2\alpha + \cos 2\beta) \end{aligned}$$

It can be verified on the basis of the solutions (5) and (7) that the boundary conditions for $\sigma_{\alpha\beta}$ and $\sigma_{\alpha\alpha}$ are indeed already approximately satisfied at small distances, of order h^2/H , from the boundary because the pressure rapidly tends to the maximum value $P_{\max} \sim \mu u_{\alpha_0} H/h^2$. The second derivatives $\partial^2 u_\alpha / \partial \beta^2$ and $\partial^2 u_\beta / \partial \beta^2$ also turn out to be small relative to the derivatives with respect to z everywhere as $\beta \rightarrow 0$. The solution (4), (7) not only satisfies the continuity equation, but also the mass balance relation

$$-\pi w_0 (AB - ab) = 4h \int_0^{\pi/2} [u_\alpha(\alpha_1, \beta) H(\alpha_1, \beta) - u_\alpha(\alpha_0, \beta) H(\alpha_0, \beta)] d\beta$$

which serves as an additional condition for the more complete problem containing the second derivatives of the velocities with respect to α and β .

This result attests to the rigor of the resulting solution within the scope of approximate thin-layer theory.

It is evident from the solution (7) that $\partial p / \partial \beta = 0$ at the outer and inner boundaries of the layer, so that for $\alpha = \alpha_0$ and $\alpha = \alpha_1$ the tangential velocity component u_β also vanishes. The contour of the cavity changes at the first instant due to the normal component u_α , which must be averaged over the layer thickness

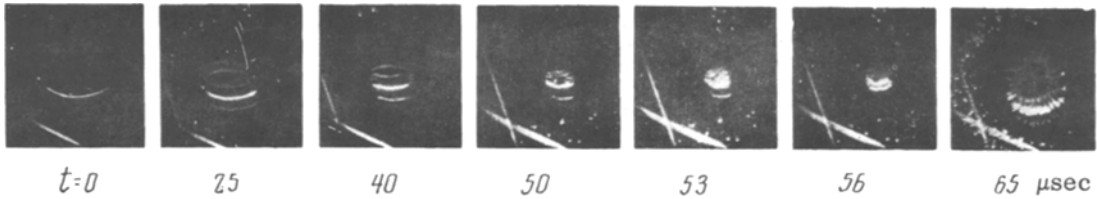


Fig. 1

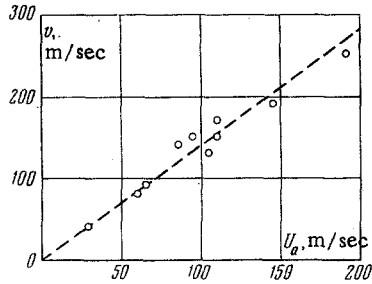


Fig. 2

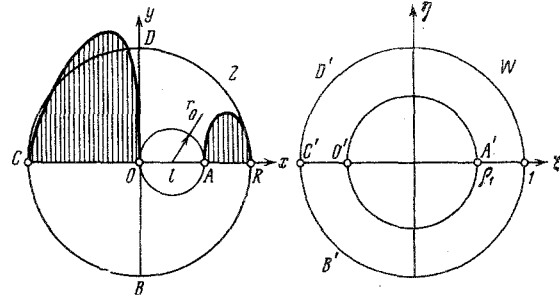


Fig. 3

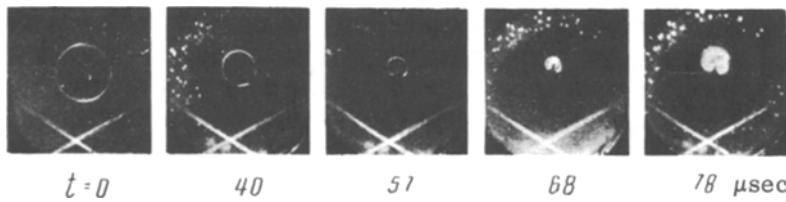


Fig. 4

$$U_{\alpha} = \frac{1}{h} \int_0^h u_x dz = - \frac{h^2}{12\mu H} \frac{\partial p}{\partial x} \quad (8)$$

If at the ensuing instants of time the shape of the contour is represented in the form

$$\Phi = \alpha - \alpha_0 + \varepsilon(\beta, t), \quad \Phi = 0$$

and the total time derivative of Φ is taken, we obtain the following equation for the cavity boundary:

$$U_{\alpha} = U_{\beta} \frac{\partial \varepsilon}{\partial \beta} + H \frac{\partial \varepsilon}{\partial t} \quad (9)$$

Using (5) and (6) for numerical calculations, we easily reduce the problem to the solution of the thermal-conduction equation with phase transition [10].

It is apparent from (7) and (8) that the velocity of the cavity boundary along α is greater than along the semiminor axis:

$$|U_{\alpha}(\alpha_0, 0)| > |U_{\alpha}(\alpha_0, \pi/2)|$$

This fact has the implication that after a certain time t_* the cavity is "punched in," or indented along the semimajor axis, gradually forming a cumulative jet. If we assume approximately that $U_{\alpha}[\alpha(t), \beta] = \text{const}$ up to the instant of indentation, we can readily estimate the time t_* from the condition for formation of an inflection point in the contour of the cavity boundary on the axis $\beta = 0$ in the form $d^2\alpha/d\beta^2 = \coth\alpha$.

We then obtain the following relation for estimation of the indentation time:

$$\begin{aligned} \frac{\tau_0}{t_*} \operatorname{sh}^2 \alpha_0 \operatorname{sh} 2\alpha_0 &= \frac{\operatorname{ch}^2 \alpha_1 - \operatorname{ch}^2 \alpha_0}{\alpha_1 - \alpha_0} - (1 + 2 \operatorname{sh}^2 \alpha_0) \operatorname{th}(\alpha_1 - \alpha_0) \\ - \operatorname{sh} 2\alpha_0 &= \frac{\delta (1 - p_1 / p_0) \operatorname{sh}^2 \alpha_0}{\alpha_1 - \alpha_0}, \quad \tau_0 = \frac{h}{|w_0|} \\ \delta &= \frac{p_0 h^3}{3\mu b^2 |w_0|}, \quad \frac{p_1}{p_0} \approx \left(\frac{a_0 b_0 h_0}{abh} \right)^{\gamma} \end{aligned} \quad (10)$$

It is convenient to use the following relations for the calculations in (10):

$$\begin{aligned} c \operatorname{ch} \alpha_0 &= a, \quad c \operatorname{sh} \alpha_0 = b, \quad c \operatorname{ch} \alpha_1 = A, \quad c \operatorname{sh} \alpha_1 = B \\ \operatorname{th}(\alpha_1 - \alpha_0) &= (aB - bA) / (Aa - Bb), \quad \alpha_1 - \alpha_0 = \ln(A + B) / (a + b) \end{aligned}$$

Photographs of the implosion of an elliptical cavity in nitroglycerin at several times are shown in Fig. 1. The experimental conditions were as follows:

$$\begin{aligned} a &= 5.0 \text{ mm}, & b &= 2.65 \text{ mm}, & h &= 0.5 \text{ mm} \\ \mu &= 0.3 \text{ p}, & p_0 &= 1 \text{ atm}, & |w_0| &= 2.5 \text{ m/sec} \end{aligned}$$

A striker in the form of a circular cylinder of radius $R = 9.5$ mm was used in the experiments. For $A \gg a$ and $B \gg b$, however, the circle can be regarded approximately as an ellipse by selecting A and B on the basis of the equal-area condition $AB = R^2$, because in this case the lengths of the semiaxes turn out to be close to R .

Figure 1 gives the first photographic evidence of the flattening of the contour along the semimajor axis at $t = 25 \mu\text{sec}$, followed by indentation and the formation of a cumulative jet at $t = 40 \mu\text{sec}$, and finally, at $t = 55 \mu\text{sec}$, detonation.

In the experiments the cumulative jet formation time t_* was measured by frame-by-frame photography. For the cases $\alpha_0 = 0.68$, $\alpha_1 = 1.6$, and $\alpha_0 = 0.72$ and $\alpha_1 = 1.6$ with $|w_0| = 1-4$ m/sec the dimensionless times t_*/τ_0 at which jet formation began turned out to be 0.19 and 0.148. Calculations according to Eq. (10) yield values of $t_*/\tau_0 = 0.38$ and 0.26. During implosion the value of U_α increases, so that the lower limit of t_*/τ_0 can be determined by substituting the value of α_0^* at the instant of indentation into (10). This correction for $\alpha_0^* = 0.54$ yields respective values of 0.18 and 0.1 for t_*/τ_0 , i.e., satisfactory agreement with the experimental.

In accordance with similarity theory [11], Eq. (10) does not include the Reynolds number, because Eqs. (1) and (2) do not contain the density. The dependence on Re shows up when the inertial terms are included [12]. The experiment also indicates a weak dependence on Re .

The experimental data on the maximum jet velocity V as a function of the cavity boundary velocity U_a along the axis a at the indentation time are given in Fig. 2. The experimental conditions were as follows: $R = 9.5$ mm; various values of $h_0 = 0.25$ to 1.0 mm; $|w_0| = 1-4$ m/sec; $2a = 7.5-10$ mm; and $2b = 4-5$ mm.

The approximate dependence $V \approx 1.4U_a$ is inferred from Fig. 2. Using (7) and (8), we express the velocity ratio at the indentation time and compare it with the experimental, which gives values of 1.9 and 2.0 for U_a/U_b in the cases $\alpha_0 = 0.68$, $\alpha_1 = 1.6$, and $\alpha_0 = 0.72$, $\alpha_1 = 1.89$, respectively. If we assume that the elliptical cavity retains its shape during the implosion process, at time $t = t_*$ the theory gives approximately 1.4 and 1.55. At the initial time the values of U_a/U_b calculated according to (7) and (8) are, respectively, 1.25 and 1.40.

We now consider the indentation of a circular cavity of radius r_0 displaced a distance l relative to the center of the striker. We map the doubly connected domain (Fig. 3) onto a canonical domain [13, 14] by means of the fractional-linear function

$$\begin{aligned} w &= \frac{R - \omega z}{z - \omega R}, \quad \rho_1 = \frac{R - \omega(l + r_0)}{l + r_0 - \omega R}, \quad w = \xi + i\eta \\ 2Rl\omega &= R^2 + l^2 - r_0^2 + [(R^2 + l^2 - r_0^2)^2 - 4R^2 l^2]^{1/2} \end{aligned} \quad (11)$$

which takes the points $z = \pm R$ and $z = l \pm r_0$ into the points $w = \pm 1$ and $w = \pm \rho_1$, respectively.

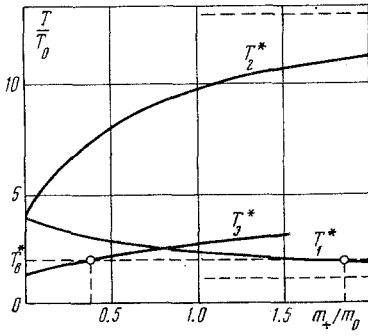


Fig. 5

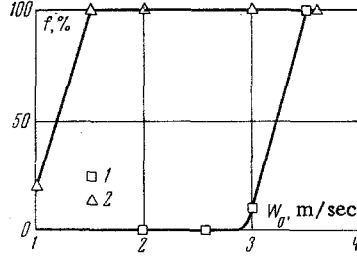


Fig. 6

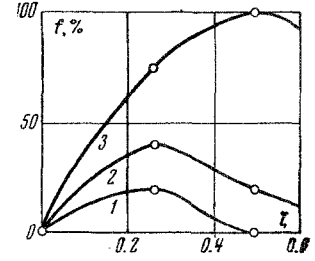


Fig. 7

We solve the problem of determining the pressure fields

$$p = P + p_1, \quad p_1 = -\frac{K}{4}(x^2 + y^2 - R^2), \quad \rho \frac{\partial}{\partial \rho} \rho \frac{\partial P}{\partial \rho} + \frac{\partial^2 P}{\partial \theta^2} = 0$$

$$P(1, \theta) = 0, \quad P(\rho_1, \theta) = \frac{1}{4}K(r_0^2 - l^2 - R^2 + 2lX), \quad K = \frac{12\mu |w_0|}{h^3}$$

$$X = \frac{R(1 + \omega^2)}{2\omega} + \frac{R(1 - \omega^2)(\omega^2 - \rho_1^2)}{2\omega\rho_1^2(1 + \lambda^2 - 2\lambda \cos \theta)}, \quad \lambda = -\frac{\omega}{\rho_1} < -1$$

$$\theta = \arctg \eta / \xi, \quad \rho^2 = \xi^2 + \eta^2$$

in the series

$$\frac{4p}{K} = R^2 - x^2 - y^2 + \left[\frac{2Rl}{\omega} + r_0^2 - l^2 - R^2 \right] \frac{\ln r}{\ln \rho_1}$$

$$+ \frac{2Rl(1 - \omega^2)}{\omega} \sum_{n=1}^{\infty} \frac{(-1)^n (\rho^n - \rho^{-n})}{\rho_1^n - \rho_1^{-n}} \left(\frac{\rho_1}{\omega} \right)^n \cos n\theta$$

$$\xi = -\omega + \frac{R(1 - \omega^2)(x - \omega R)}{(x - \omega R)^2 + y^2}, \quad \eta = \frac{Ry(\omega^2 - 1)}{(x - \omega R)^2 + y^2}, \quad q = \ln \rho_1 \quad (12)$$

$$\frac{\partial p}{\partial x} \Big|_{x=l \pm r_0, y=0} = -2(l \pm r_0) + \frac{[2lR + \omega(r_0^2 - l^2 - R^2)](1 - \omega^2)R}{\rho_1 \omega \ln \rho_1 (l \pm r_0 - \omega R)^2}$$

$$+ \frac{2lR^2(1 - \omega^2)^2}{\omega(l \pm r_0 - \omega R)^2} \sum_{n=1}^{\infty} \frac{(\mp 1)^n n \operatorname{cth} qn}{\omega^n}$$

The substitution of $\rho(x,y)$ and $\theta(x,y)$ into equations (12) yields a cumbersome expression for the determination of p .

For the calculation of p and $\operatorname{grad} p$ at the characteristic points, however, it is convenient to use (12) directly, taking the correspondence of points in the z and w planes into account. The pressure curve for a liquid with a displaced cavity is plotted qualitatively in Fig. 3.

It follows from (12) that $|\partial p / \partial x|_{l - r_0} > (\partial p / \partial x)_{l + r_0}$, so that indentation and the formation of a cumulative jet begins from the side nearest the center of the striker. This situation is also physically reasonable insofar as the pressure maximum occurs at the center in the absence of the cavity [15, 16].

Frame-by-frame photographs through a magnifying glass of the implosion process for a displaced cavity are given in Fig. 4. Under the experimental conditions $h = 0.5$ mm, $r_0 = 3.5$ mm, $R = 9.5$ mm, and $l = 1.3$ mm.

The unidirectional indentation of the cavity at $t_* = 57$ μsec and its transport with the flow are clearly seen in Fig. 4. At $t = 68$ μsec the nitroglycerin ignites and detonates.

The majority of experiments on the impact sensitivity of nitroglycerin are readily explained by an analysis after Johansson [4] of a graph of the cavity surface temperature as a function of the ratio of the mass m_+ of burning droplets to the mass m_0 of the gas in the cavity with allowance for the dependence of m_+ on the mass and velocity of the cumulative jet.

Relying on the degree of compression $\sigma = h_0 r_0^2 / h_* r_*^2 \approx 65$ attained by the cavity experimentally, we plotted the graph of Fig. 5, in which T_1 is the temperature of the compressed gas with regard for cooling due to heating of the droplets, T_2 is the temperature after combustion of all the heated droplets of mass m_+ ,

T_3 is the temperature of the liquid at the cavity boundary in this case, and T_b (dashed curve) is the ignition temperature calculated for a detonation delay time of 10^{-5} sec, which corresponds to the transit time of the droplets across the cavity. The T_1 and T_2 curves were plotted on the basis of energy balance considerations, and T_3 was calculated as the temperature at the boundary for the contact of two unequally heated semi-infinite bodies:

$$\frac{T_1}{T_0} = \frac{c_0 m_0 \sigma^{\gamma-1} + c_+ m_+}{c_0 m_0 + c_+ m_+}, \quad T_2 = T_1 + \frac{Q m_+}{(m_0 + m_+) c_p}$$

$$\frac{T_3}{T_0} = \frac{1 + \alpha T_2 / T_0}{1 + \alpha}, \quad \alpha^2 = (\lambda c \rho)_1 / (\lambda c \rho)_0, \quad T^* = \frac{T}{T_0}$$

Here Q is the heat of reaction, $\gamma = 1.3$ is the adiabatic exponent, c is the heat capacity, λ is the thermal conductivity, and the subscript 1 refers to the products of detonation. We see from Fig. 5 that for a small number of droplets the temperature at the cavity wall is close to the temperature determined by the thermal conductivity from an adiabatically heated gas, and for degrees of compression $\sigma \leq 65$ detonation does not take place. If the number of droplets is relatively large, the temperature T_1 of the actual gas in the cavity falls below the ignition temperature of the liquid. Consequently, the optimum segment of the curve for the development of detonation is $0.4 \leq m_+ / m_0 \leq 1.8$.

Similarity considerations [11] imply that the droplet spectrum is characterized by the complex relation

$$m_+ = h r_+^2 \rho_+ F\left(\frac{d_0}{h}, \frac{\rho_0 d_0 V^2}{\sigma_0}, \frac{\rho_+ V d_0}{\mu}, \frac{r_+}{h}, \Omega\right)$$

in which m_+ is the mass of liquid droplets ranging from molecular diameters (vapor) to the instantaneous diameter d_0 , Ω is the angle of impact of the cumulative jet on the liquid at the cavity boundary, and σ_0 is the surface tension. Inasmuch as the form of the function F is unknown, we can estimate d_0 with the aid of the Weber criterion $\rho_0 V^2 d_0 / \sigma_0 \leq 10$, from which it follows that the experimentally observed maximum droplet diameter for $\rho_0 \approx 10^{-2}$ g/cm³, $\sigma_0 = 50$ dyn/cm, and $V = 10^4$ cm/sec was $d_0 \leq 5 \cdot 10^{-4}$ cm. Drops of this size can become heated during the transit time across the cavity, $t_+ \approx 2r_+ / V$, since for $r_+ \approx 0.1$ cm and the thermal conductivity of nitroglycerin, $\kappa \sim 10^{-3}$ cm²/sec, the heating time $d_0^2 / \pi^2 \kappa \leq t_+$.

The results of an experimental comparison of the frequency of detonations with a central circular cavity ($r_0 = 2.5$ mm, $R = 9.5$ mm, $h_0 = 0.5$ mm) and an elliptical cavity having the same initial volume $hab = h_0 r_0^2$ and $a \approx 2b$ are shown in Fig. 6 (curves 1 and 2, respectively). Notice the sharp increase in the detonation frequency due to intensification of the cumulative effect and, hence, due to the increase in m_+ / m_0 (see Fig. 5).

A graph of the detonation frequency for a circular cavity of the same dimensions as in Fig. 6 versus the displacement $\xi = l/R$ of its center for various impact velocities $|w_0| = 2, 2.5,$ and 3 m/sec is given in Fig. 7 (curves 1, 2, and 3, respectively). An increase in ξ , which causes the velocity of the cumulative jet to increase, at first increases the detonation frequency, but then a decrease of f with increasing ξ is observed, a result that is explained by the experimentally observed smearing out of the bubbles beyond the limits of the striker.

We note in conclusion that the local heating of the liquid behind the shock front with the introduction of the cumulative jet is small.

Assuming for the purpose of estimation that the total internal energy behind the wave front is thermal, $\Delta T < (u + V)^2 / 8c_v$, for standard experimental conditions in which $u + V \leq 300$ m/sec and $c_v \approx 0.2$ cal/g^oK we obtain a temperature increase of order 10° K.

We now show that viscous heating of the liquid at the zone of contact of the cavity and striker surface also fails to produce ignition. We infer from the solution [9] pertaining to the indentation of a circular layer of viscous liquid that the velocity gradient

$$\frac{\partial u}{\partial z} = \frac{3w_0 R}{h^3} (2z - h) \frac{y \ln \xi + 1 - \xi}{V y \ln \xi}, \quad h = h_0 \frac{1 + \beta \ln \beta - \beta}{1 + \xi \ln \xi - \xi}$$

$$\xi = \frac{r_+^2}{R^2} < 1, \quad \beta = \frac{r_0^2}{R^2}, \quad y = \frac{r^2}{R^2} \quad (13)$$

is a maximum for $z = 0$ and $z = h$ at the points $y = 1$ and $y = \xi$, where $(\partial u / \partial z)_{y=1} < (\partial u / \partial z)_{y=\xi}$.

The maximum temperature increase without consideration of the thermal conductivity is determined by the energy dissipation

$$\rho c_p \frac{\partial T}{\partial t} = \mu \left(\frac{\partial u}{\partial z} \right)_{y=\xi}^2, \quad \frac{\partial T}{\partial t} = w_0 \frac{\partial T}{\partial h} \frac{\partial h}{\partial \xi}$$

Taking (13) into account, we find

$$\Delta T = \frac{E}{(1 + \beta \ln \beta - \beta)^3} \int_{\beta}^{\xi} \frac{(1 + \xi \ln \xi - \xi)^4}{\xi \ln \xi} d\xi \quad (14)$$

$$E = 9\mu w_0 R^2 / \rho c_p h_0^3$$

Inasmuch as $-1 < \xi \ln \xi - \xi < 0$, we deduce the following by majorization of the integrand of (14):

$$\Delta T \leq \frac{E}{(1 + \beta \ln \beta - \beta)^3} \ln \frac{\ln \beta}{\ln \xi}$$

i.e., the viscosity causes the temperature in the liquid to increase very slowly, the increment amounting to about 20° for characteristic experimental conditions ($\beta = 0.25$, $\xi = 4 \cdot 10^{-3}$).

LITERATURE CITED

1. F. P. Bowden and A. D. Yoffe, *Fast Reactions in Solids*, Butterworths, London (1958).
2. E. I. Zababakhin, "Energy accumulation and its limits," *Usp. Fiz. Nauk*, **85**, No. 4, 721 (1965).
3. R. I. Soloukhin, "The bubble mechanism of impact ignition in liquids," *Dokl. Akad. Nauk SSSR*, **136**, No. 2 (1961).
4. C. H. Johansson, "The initiation of liquid explosives by shock and the importance of liquid breakup," *Proc. Roy. Soc., Ser. A*, **246**, No. 1245 (1958).
5. C. H. Johansson and H. L. Selberg, "The ignition mechanism of high explosives," *Appl. Sci. Res., Ser. A*, **5**, No. 6 (1956).
6. V. K. Boblev and A. V. Dubovik, "Cumulative jets in the impact-initiated implosion of cavities in thin liquid layers," *Zh. Prikl. Mekhan. i Tekh. Fiz.*, No. 2 (1970).
7. M. I. Kornfel'd, *Elasticity and Strength of Liquids* [in Russian], Gostekhteorizdat, Moscow-Leningrad (1951).
8. M. A. Lavrent'ev, "The cumulative charge and its operating principles," *Usp. Matem. Nauk*, **12**, No. 4, 76 (1957).
9. É. I. Andriankin, V. K. Bobolev, and A. V. Dubovik, "Impact-initiated implosion of a cylindrical cavity in a liquid layer," *Zh. Prikl. Mekhan. i Tekh. Fiz.*, No. 6 (1970).
10. A. N. Tikhonov and A. A. Samarskii, *Equations of Mathematical Physics*, Pergamon (1964).
11. L. I. Sedov, *Similarity and Dimensional Methods in Mechanics*, Academic Press (1959).
12. É. I. Andriankin, "Breakup of a viscous drop in impact," *Zh. Prikl. Mekhan. i Tekh. Fiz.*, No. 5, 142 (1966).
13. M. A. Lavrent'ev and B. V. Shabat, *Methods of the Theory of Functions of a Complex Variable* [in Russian], Fizmatgiz, Moscow (1958).
14. M. V. Keldysh, "Conformal mapping of multiconnected domains onto canonical domains," *Usp. Matem. Nauk*, No. 6, 90 (1939).
15. G. I. Pokrovskii, *Detonation* [in Russian], Nedra, Moscow (1964).
16. V. K. Kedrinskii and R. I. Soloukhin, "Compression of a spherical gas bubble by a shock wave in water," *Zh. Prikl. Mekhan. i Tekh. Fiz.*, No. 1, 27 (1961).